### Title

Characterization and Evaluation of 64Cu-Labeled A20FMDV2 Conjugates for Imaging the Integrin αvβ6




### Journal

Molecular Imaging and Biology, 16(4)

### ISSN

1536-1632



### Authors

Hu, Lina Y
Bauer, Nadine
Knight, Leah M
et al.



### Publication Date

2014-08-01

### DOI

10.1007/s11307-013-0717-9

Peer reviewed

Published in final edited form as:
*Mol Imaging Biol*. 2014 August ; 16(4): 567–577. doi:10.1007/s11307-013-0717-9.

# Characterization and Evaluation of $^{64}$Cu-Labeled A20FMDV2 Conjugates for Imaging the Integrin $\alpha_v\beta_6$

**Lina Y. Hu**[1], **Nadine Bauer**[1], **Leah M. Knight**[1], **Zibo Li**[2], **Shuanglong Liu**[2], **Carolyn J. Anderson**[3], **Peter S. Conti**[2], and **Julie L. Sutcliffe**[1,4,5]

[1]Department of Biomedical Engineering, University of California Davis, Davis, CA, USA

[2]Department of Radiology, University of Southern California, Los Angeles, CA, USA

[3]Department of Radiology, University of Pittsburgh, Pittsburgh, PA, USA

[4]Department of Internal Medicine, Division of Hematology/Oncology, University of California Davis, School of Medicine, Research II, 4625 2nd Ave, Sacramento CA, 95817, USA

[5]Center for Molecular and Genomic Imaging, University of California Davis, Davis, CA, USA

## Abstract

**Purpose—**The integrin $\alpha_v\beta_6$ is overexpressed in a variety of aggressive cancers and serves as a prognosis marker. This study describes the conjugation, radiolabeling, and *in vitro* and *in vivo* evaluation of four chelators to determine the best candidate for $^{64}$Cu radiolabeling of A20FMDV2, an $\alpha_v\beta_6$ targeting peptide.

**Procedures—**Four chelators were conjugated onto $PEG_{28}$-A20FMDV2 (1): 11-carboxymethyl-1,4,8,11-tetraazabicyclo[6.6.2]hexadecane-4-methanephosphonic acid (CB-TE1A1P), 1,4,7,10-tetraazacyclododecane-1,4,7,10-tetraacetic acid (DOTA), 1,4,7-triazacyclononane-1,4,7-triacetic acid (NOTA), and 4,4′-((3,6,10,13,16,19-hexazabicyclo[6.6.6]ico-sane-1,8-diylbis(aza-nediyl)) bis(methylene)dibenzoic acid (BaBaSar). All peptides were radiolabeled with $^{64}$Cu in ammonium acetate buffer at pH 6 and formulated to pH 7.2 in PBS for use. The radiotracers were evaluated using *in vitro* cell binding and internalization assays and serum stability assays. *In vivo* studies conducted include blocking, biodistribution, and small animal PET imaging. Autoradiography and histology were also conducted.

**Results—**All radiotracers were radiolabeled in good radiochemical purity (>95 %) under mild conditions (37–50 °C for 15 min) with high specific activity (0.58–0.60 Ci/μmol). All radiotracers demonstrated $\alpha_v\beta_6$-directed cell binding (>46 %) with similar internalization levels (>23 %). The radiotracers $^{64}$Cu-CB-TE1A1P-1 and $^{64}$Cu-BaBaSar-1 showed improved specificity for the $\alpha_v\beta_6$ positive tumor *in vivo* over $^{64}$Cu-DOTA-1 and $^{64}$Cu-NOTA-1 (+/− tumor uptake ratios—3.82 +/



*Correspondence to:* Julie L. Sutcliffe; jlsutcliffe@ucdavis.edu.

Electronic supplementary material The online version of this article (doi:10.1007/s11307-013-0717-9) contains supplementary material, which is available to authorized users.

*Conflict of Interest.* No conflicts of interest exist.

−0.44, 3.82±0.41, 2.58±0.58, and 1.29±0.14, respectively). Of the four radiotracers, $^{64}$Cu-NOTA-1 exhibited the highest liver uptake (10.83±0.1 % ID/g at 4 h).

**Conclusions—**We have successfully conjugated, radiolabeled, and assessed the four chelates CB-TE1A1P, DOTA, NOTA, and BaBaSar both *in vitro* and *in vivo*. However, the data suggests no clear "best candidate" for the $^{64}$Cu-radiolabeling of A20FMDV2, but instead a trade-off between the different properties (e.g., stability, selectivity, pharmacokinetics, etc.) with no obvious effects of the individual chelators.

### Keywords

Integrin $\alpha_v\beta_6$; Copper-64; PET imaging

## Introduction

The integrin $\alpha_v\beta_6$ is an epithelial-specific receptor that is emerging as a biologically and clinically relevant target for the molecular imaging of cancer [1]. This integrin is not expressed in the vast majority of healthy adult epithelium but has been shown to be significantly upregulated in a variety of cancers including oral squamous cell carcinoma, intestinal gastric carcinoma, ovarian cancer, and pancreatic ductal adenocarcinoma [2–5]. Additionally, it serves as a prognostic indicator with high levels of expression correlating with poor patient prognosis [6, 7]. A molecular imaging agent that targets the integrin $\alpha_v\beta_6$ could lead to new diagnostic and therapeutic strategies to improve the overall prognosis of the disease [8, 9].

Imaging agents in the form of radiolabeled peptides have been used to image $\alpha_v\beta_6$ since they are relatively easy to synthesize with flexibility for chemical modifications while maintaining high binding affinity and specificity [10–13]. We have previously shown that the 20-amino acid peptide A20FMDV2 can selectively target $\alpha_v\beta_6$ in a human tumor xenograft mouse model using the cell line DX3puroβ6, a human melanoma cell line expressing $\alpha_v\beta_6$ [14]. We have also shown that the addition of a monodisperse polyethylene glycol (PEG) polymer onto A20FMDV2 improves its pharmacokinetics and *in vivo* stability [15]. A20FMDV2 has been conjugated to 4,11-bis(carboxymethyl)-1,4,8,11-tetraaza-bicyclo[6.6.2]hexadecane (CB-TE2A) and monocyclic 1,4,7,10-tetraazacyclododecane-1,4,7,10-tetraacetic acid (DOTA) for radiolabeling with copper-64 to make the radiotracer more suitable for therapy as $^{64}$Cu has both $\beta^+$ (20 %) and $\beta^-$ (37 %) emissions [16, 17]. While this work showed successful radiolabeling and small animal imaging with PET (positron emission tomography), both peptides exhibited high kidney retention and the CB-TE2A-conjugated peptide required high temperatures for $^{64}$Cu incorporation, leaving much room for optimization for both radiolabeling and pharmacokinetics.

This study evaluates four $^{64}$Cu chelators and their effects on the *in vitro* and *in vivo* properties of the pegylated A20FDMV2 peptide: 11-carboxymethyl-1,4,8,11-tetraazabicyclo[6.6.2] hexadecane-4-methanephosphonic acid (CB-TE1A1P), DOTA, 1,4,7-triazacyclononane-1,4,7-triacetic acid (NOTA), and 4,4′-((3,6,10,13,16,19-hexazabicyclo[6.6.6]ico-sane-1,8-diylbis (aza-nediyl))bis(methylene)dibenzoic acid

(BaBaSar). CB-TE1A1P is a cross-bridged macrocycle with a methane phosphonic acid pendant arm that can be radiolabeled under mild conditions while exhibiting high kinetic stability when conjugated to the peptidomimetic LLP2A [18]. DOTA and NOTA are both widely used, commercially available chelators. BaBaSar is a carboxyl-functionalized sarcophagine cage-based chelator that can also be radiolabeled under mild conditions and exhibited lower liver uptake compared to DOTA when conjugated to a cyclic RGD peptides [19, 20]. Here we describe the conjugation, radiolabeling, and *in vitro* and *in vivo* characterizations of all four tracers to determine the best candidate for $^{64}$Cu radiolabeling of pegylated A20FMDV2.

## Materials and Methods

Solvents and chemicals were purchased from Aldrich (Milwaukee, WI, USA) unless stated otherwise and used without further purification. 9-Fluorenylmethoxycarbonyl (Fmoc)-protected amino acids, Novasyn TGR resin, Fmoc-NH-$PEG_{28}$-carboxylic acid, and coupling reagents were purchased from NovaBiochem (San Diego, CA, USA) or GL Biochem (Shanghai, China). The chelators DOTA($t$Bu)$_3$ and NOTA($t$Bu)$_2$ were purchased from CheMatech (Dijon, France). A reverse-phase high-performance liquid chromatography (HPLC; Beckman Coulter Gold HPLC) system was used to analyze and purify the peptides. The system has an ultraviolet absorbance detector (220 nm) and a radioactivity detector (photomultiplier tube; Flow-Count radio-HPLC system, Bioscan, Washington DC, USA) connected in series. The mobile phase was 0.05 % trifluoroacetic acid in water (v/v; solvent A) and 100 % acetonitrile (solvent B). For the analytical HPLC: Phenomenex Jupiter 4μ Proteo 90 Å column (250×4.6 mm, 4 μm), solvent B isocratic 9 % for 2 min, then a linear gradient to 81 % over 30 min with a flow rate of 1.5 ml/min. For the semi-preparative HPLC: Phenomenex Jupiter 10 μ Proteo 300 Å column (250×10 mm, 10 μm), solvent B isocratic 9 % for 2 min, then a linear gradient to 81 % over 30 min at a flow rate of 3 ml/min. Mass spectrometry was performed using an ABI 4700 matrix-assisted laser desorption-ionization time of flight/time of flight (MALDI TOF/TOF) spectrometer (Applied Biosystems, Foster City, CA, USA).

The cell lines DX3puro and DX3puroβ6 were described previously [14]. The cells were cultured at 37 °C and 5 % $CO_2$ in Dulbecco's Modified Eagle's Medium (DMEM) containing 10% fetal bovine serum and 1 % penicillin–streptomycin–glutamine (Gibco/Life Technologies, Grand Island, NY, USA). All immunohistochemistry supplies were purchased from Vector Labs (Burlingame, CA, USA) unless otherwise stated.

Cell labeling and biodistribution samples were analyzed with a Wizard 1470 gamma counter (Perkin-Elmer, Waltham, MA, USA). Small-animal PET scans were acquired on a Siemens Inveon DPET scanner and computed tomography (CT) scans on a combined high-resolution Inveon SPECT/CT system (Siemens Medical Solutions USA, Knoxville, TN, USA). The data was processed with Siemens Inveon Research Workplace software.

### Peptide Synthesis

The 20-mer A20FMDV2 peptide was manually synthesized on Novasyn TGR resin using three molar equivalents of amino acids and *O*-(7-azabenzotriazol-1-yl)-*N*,*N*,*N*′,*N*′-

tetramethyluronium hexafluorophosphate (HATU) and six molar equivalents of *N*-diisopropyslethylamine (DIPEA) for 1.5-h coupling time at room temperature followed by 30 min total of Fmoc deprotection with 20 % piperidine in *N*,*N*-dimethylformamide (DMF). The peptide was modified using Fmoc–$PEG_{28}$–COOH as reported previously [16]. The chelators DOTA($t$Bu)$_3$ and NOTA($t$Bu)$_2$ were coupled onto the pegylated peptide (1) using 3 molar equivalents for 3 h at room temperature to create the tracers DOTA-1 and NOTA-1, respectively. CB-TE1A1P was similarly coupled on solid phase using 6 molar equivalents overnight at room temperature to yield CB-TE1A1P-1. Peptide conjugates on solid phase were cleaved from the resin using trifluoroacetic acid/1,2-ethanedithiol/triisopropyl-silane/water 94:2.5:1:2.5 (v/v/v/v) to yield the C-terminus amides. The crude peptide conjugates were dissolved in water and washed three times with diethyl ether before analysis with HPLC and MALDI. BaBaSar was conjugated onto the cleaved pegylated peptide with Lys(ivDde) in solution phase to create BaBaSar-1 (Fig. 1). Briefly, the carboxylic acid on BaBaSar was activated by ethyl(dimethylaminopropyl) carbodiimide and sulfo-*N*-hydroxysulfosuccinimide to form a BaBaSar–Osu intermediate. Without purification, BaBaSar–Osu was conjugated with the free amino group on the peptide. The ivDde protecting group was later removed using 2 % hydrazine in DMF (v/v) for 30 min at room temperature, followed by HPLC and MALDI. All peptide conjugates were purified using semipreparative HPLC prior to radiolabeling.

## Radiochemical Synthesis

Copper-64 was obtained from Washington University School of Medicine in the form $^{64}CuCl_2$ (5–10 μl in 0.5 M HCl) and diluted in ammonium acetate buffer (pH 6). All four peptide conjugates (CB-TE1A1P-1, DOTA-1, NOTA-1, and BaBaSar-1) were dissolved in sterile ammonium acetate buffer before radiolabeling to a final concentration of 10 mg/ml. Each peptide (0.25 mg, 25 μl) was added to $^{64}$Cu-acetate (4–7 mCi) with a final volume of 50–60 μl in 0.1 M ammonium acetate buffer (pH 6). All reactions were carried out at 37 °C for 15 min, except for CB-TE1A1P-1, which was radiolabeled at 50 °C for 15 min. The radiochemical purity (RCP) of each reaction was determined using HPLC after quenching an aliquot of the reaction with 5 mM ethylenediaminetetraacetic acid (EDTA, 150 μl).

## In Vitro Experiments

**Cell Binding—**Cell lines were analyzed with flow cytometry before experiments to confirm integrin expression levels. Cell binding experiments were carried out as previously described [21]. Briefly, 4 μCi of each radiotracer was added to a cell suspension of either DX3puro ($\alpha_v\beta_6$ negative) or DX3puroβ6 ($\alpha_v\beta_6$ positive) cells in serum-free DMEM (pH 7.2; $3.75\times10^6$ cells in 50 μl) in Eppendorf tubes pretreated with bovine serum albumin (5 % wt/v in PBS) to block non-specific binding. The mixture was incubated at room temperature with regular agitation for 60 min before washing with serum-free DMEM. Following centrifugation (130×*g*, 3 min), the supernatant was separated from the cell pellet. The pellet underwent an additional wash with 0.5 ml serum-free DMEM, and the supernatants were combined before the fraction of bound activity was determined with a gamma counter. To determine the fraction of internalized radiotracer, the cells were treated with cold acidic wash buffer (pH 2.5, 300 μl) for 5 min at 4 °C, centrifuged (130×*g*, 3 min), and washed with

0.3 ml cold PBS. The supernatants were then combined and the cells were subsequently re-suspended in 0.6 ml PBS. The internalized fraction was detected with a gamma counter and expressed as a percentage of total activity.

**Serum Stability—**Mouse serum was combined with an aliquot of the formulated radiotracer (100–200 μCi) and incubated at 37 °C. At time points of 1, 4, and 24 h, aliquots (100–200 μl) were taken from the sample, mixed with absolute ethanol (500 μl, 4 °C), and centrifuged (2,300×*g*, 2.5 min) to precipitate out serum proteins. The supernatant was challenged with 5 mM EDTA solution (300 μl) before HPLC analysis to determine the fraction of intact radiotracer.

## In Vivo Experiments

Female *nu*/*nu* nude mice (6–8 weeks old) were purchased from Charles River Laboratories (Wilmington, MA, USA) and handled according to the UC Davis Institutional Animal Care and Use Committee. DX3puro and DX3puroβ6 cells ($3\times10^6$) in 100 μl serum-free DMEM were implanted subcutaneously into opposite shoulder flanks and allowed to grow for approximately 3 weeks (0.5–1 cm in diameter). All cells were evaluated with flow cytometry before injection to confirm integrin expression levels. Food and water were available *ad libitum*.

## Small-Animal Imaging

Aliquots of the formulated radiotracer (150–250 μCi in 50–60 μl) in isotonic solution (pH 7.2) were injected intravenously (i.v.) via a catheter into the tail vein of mice (*n*=4/time point/radiotracer) anesthetized with 2–3 % isoflurane in medical grade oxygen. Animals were imaged two at a time, side by side in a feet-first prone position on the scanner bed. For blocking studies, $NH_2$-$PEG_{28}$-A20FMDV2 (30 mg/kg as a 10 mg/ml solution in PBS) was injected 10 min before the formulated radiotracer. Anesthesia was maintained during the scan at 1.5–2.5 % isoflurane in medical-grade oxygen. Static, single-frame 15-min emission scans were acquired at time points of 1, 4, and 24 h post-injection (p.i.). A cobalt-57 transmission scan for attenuation correction and a CT scan for anatomical reference were also acquired.

## Autoradiography and Histology

Each formulated radiotracer (1 mCi in 200 μl) was injected into the tail vein of a mouse (*n*=1/radiotracer). Following a 4-h conscious uptake time, the mouse was anesthetized and sacrificed. Both tumors and the kidneys were dissected and frozen in freezing medium (Tissue-Tek, Sakura Finetek). The tissues were sectioned using a Leica CM1850 cryostat (Leica Microsystems) in 20-μm slices and exposed to a storage phosphor screen (GE Healthcare) overnight. The screen was read with a Storm 860 phosphorimager (GE Healthcare) using a 50-μm resolution.

For immunohistochemistry staining, tumors were sectioned into 5-μm slices and mounted onto glass slides (3 sections/slide). The slides were fixed with periodate–lysine–paraformaldehyde, washed with PBS, and outlined with an ImmEdge pen. Endogenous peroxidase was blocked using 3 % hydrogen peroxide and 0.3 % normal horse serum in

PBS. To block non-specific uptake, 2.5 % normal horse serum was used prior to antibody binding steps. The antibodies used were an anti-integrin β6 antibody (Santa Cruz Biotechnologies, Inc., Dallas, TX, USA) for 1 h at room temperature and a subsequent HRP-labeled anti-goat antibody for 30 min at room temperature. Negative controls were performed for each tumor omitting the primary antibody. The substrate used was ImmPACT DAB and the enzymatic reaction was stopped after 10 min with water. Mayer's hematoxylin was used as the background stain (30 s, room temperature) and washed with water. The slides were then dehydrated in ethanol (70, 95, and 100 %), followed by xylene (100%, twice) and permanently mounted with DePEX mounting medium.

### Biodistribution

Aliquots of the formulated radiotracer (50 μCi in 50–60 μl isotonic solution) were injected into the tail vein followed by conscious uptake periods of 1, 4, and 24 h. At each time point, the mice ($n$=3/time point/radiotracer) were anesthetized and sacrificed. The tissues were collected, rinsed with PBS, and the radioactivity of each measured with a gamma counter. Radioactivity concentrations were calibrated, decay-corrected, and expressed as percent of injected dose per gram of tissue (% ID/g).

### Urine Analysis

Urine samples (10–100 μl, $n$=1/time point/radiotracer) were collected during biodistribution studies at 1 and 4 h p.i. and analyzed for degradation by radioHPLC. Proteins were precipitated with absolute ethanol (500 μl, 4 °C) and removed by centrifugation at 2,300×$g$ for 10 min. All samples were challenged with 5 mM EDTA solution (300 μl) before HPLC analysis.

### Statistical Analysis

All statistical data are reported as mean±standard deviation (SD). Paired, two-tailed Student's $t$ tests were used to evaluate statistical significance, where $p$ <0.05 was considered statistically significant.

## Results

### Peptide Synthesis

The tracers were prepared as described and obtained in high purity (≥95 %). The analytical data for the peptides are as follows: CB-TE1A1P-1, HPLC retention time ($R_t$)=16.1 min; MALDI $m/z$=3,827.3, calculated ($C_{167}H_{310}N_{37}O_{60}P$)=3,827.5; DOTA-1, HPLC $R_t$=16.3 min; MALDI $m/z$=3,852.1, calculated ($C_{168}H_{307}N_{37}O_{63}$)=3,852.2; NOTA-1, HPLC $R_t$=14.9 min; MALDI $m/z$=3,752.2, calculated ($C_{164}H_{300}N_{36}O_{61}$)=3,752.3; BaBaSar-1, HPLC $R_t$=14.3 min; MALDI $m/z$=4,031.9, calculated ($C_{182}H_{325}N_{41}O_{59}$)=4031.8 (Table 1).

### Radiochemical Synthesis

All peptide conjugates were incubated with $^{64}$Cu-acetate at 37 °C for 15 min with the exception of CB-TE1A1P-1 which was radiolabeled at 50 °C for 15 min. The RCP was >98 %, >95 %, >96 %, and >97 % with a specific activity of 0.58 Ci/μmol, 0.59 Ci/μmol, 0.58

Ci/μmol, and 0.60 Ci/μmol for $^{64}$Cu-CB-TE1A1P-1, $^{64}$Cu-DOTA-1, $^{64}$Cu-NOTA-1, and $^{64}$Cu-BaBaSar-1, respectively. The results are summarized in Table 1. All radiotracers were formulated to pH 7.2 in PBS without further purification.

## Cell Binding

Cell binding assays were used to evaluate the ability of the radiotracers to bind $\alpha_v\beta_6$ *in vitro*. Integrin expression in the cell lines DX3puro ($\alpha_v\beta_6$ negative) and DX3puro$\beta_6$ ($\alpha_v\beta_6$ positive) were confirmed through flow cytometry. The binding to $\alpha_v\beta_6$-positive DX3puro$\beta_6$ cells were 65.3±1.8 % for $^{64}$Cu-CB-TE1A1P-1, 60.9±1.1 % for $^{64}$Cu-DOTA-1, 46.6±1.3 % for $^{64}$Cu-NOTA-1, and 58.3±1.8 % for $^{64}$Cu-BaBaSar-1. All radiotracers demonstrated low binding to the $\alpha_v\beta_6$-negative Dx3puro cells (<12 % binding). The percent internalized relative to the amount bound to the $\alpha_v\beta_6$-positive DX3puro$\beta_6$ cells were 47.4±0.6 % for $^{64}$Cu-CB-TE1A1P-1, 46.2±1.7 % for $^{64}$Cu-DOTA-1, 40.7±3.5% for $^{64}$Cu-NOTA-1, and 23.8±1.7% for $^{64}$Cu-BaBaSar-1 (Fig. 2).

## Serum Stability

All radiotracers were incubated in mouse serum at 37 °C for 24 h with aliquots taken out at each time point. After 24 h, all radiotracers showed significant degradation with $^{64}$Cu-NOTA-1 exhibiting the highest amount of EDTA-complexed free copper (Fig. 3a).

## Small-Animal Imaging and Biodistribution

*In vivo* evaluation of $^{64}$Cu-CB-TE1A1P-1, $^{64}$Cu-DOTA-1, $^{64}$Cu-NOTA-1, and $^{64}$Cu-BaBaSar-1 by small-animal PET and biodistribution studies revealed selective uptake in the $\alpha_v\beta_6$-positive tumor over the $\alpha_v\beta_6$-negative tumor for three of the four radiotracers and renal clearance as the main route of elimination from the body for all radiotracers. At 4 h p.i., all radiotracers except $^{64}$Cu-NOTA-1 showed a statistically significant difference in uptake between the positive and negative tumors ($^{64}$Cu-CB-TE1A1P-1—$p$=0.013, $^{64}$Cu-DOTA-1—$p$=0.003, $^{64}$Cu-NOTA-1—$p$=0.475, and $^{64}$Cu-BaBaSar-1—$p$=0.015) (Fig. 4a–d). In terms of absolute % ID/g numbers, $^{64}$Cu-NOTA-1 demonstrated the highest uptake in the $\alpha_v\beta_6$-positive tumor (2.44±0.76 % ID/g at 4 h p.i.) and $^{64}$Cu-DOTA-1 demonstrated the lowest uptake in the $\alpha_v\beta_6$-positive tumor (1.11±0.58 % ID/g at 4 h p.i.) (Table 2). However, positive to negative tumor ratios reveal that $^{64}$Cu-CB-TE1A1P-1 and $^{64}$Cu-BaBaSar-1 had the highest specificity for the $\alpha_v\beta_6$-positive tumor (3.82±0.44 and 3.82±0.41, respectively) (Fig. 4e). All radiotracers exhibited high kidney uptake at 4 h p.i. with $^{64}$Cu-BaBaSar-1 (196.9±54.5 % ID/g) and $^{64}$Cu-CB-TE1A1P-1 (122.7±25.8 % ID/g) having higher kidney uptake than $^{64}$Cu-DOTA-1 (69.2±11.8 % ID/g) and $^{64}$Cu-NOTA-1 (69.12±19.5 % ID/g) (Fig. 5b). All four radiotracers had relatively low liver uptake with $^{64}$Cu-NOTA-1 having the highest liver uptake (10.8±1.1 % ID/g) and $^{64}$Cu-CB-TE1A1P-1 having the lowest liver uptake and that stayed consistently low at all time points (1 h—1.27±0.17 % ID/g, 4 h—1.45±0.14 % ID/g, 24 h—0.92±0.8 % ID/g) (Fig. 5c). Both $^{64}$Cu-DOTA-1 (1 h—2.04±0.33 % ID/g, 4 h—1.41±0.57 % ID/g, 24 h—3.13±0.43 % ID/g) and $^{64}$Cu-BaBaSar-1 (1 h—1.54±0.23 % ID/g, 4 h—2.61±0.05 % ID/g, 24 h—3.41±0.35 % ID/g) showed a slightly increasing trend from 1 to 24 h p.i. Uptake in other non-target organs such as gallbladder (24 h—$^{64}$Cu-CB-TE1A1P-1, 1.84±1.15 % ID/g; $^{64}$Cu-DOTA-1, 2.26±0.35 % ID/g; $^{64}$Cu-

NOTA-1, 1.45±0.24 % ID/g; and $^{64}$Cu-BaBaSar-1, 3.43±0.36 % ID/g) and stomach (24 h—$^{64}$Cu-CB-TE1A1P-1, 7.35±1.48 % ID/g; $^{64}$Cu-DOTA-1, 5.34±0.96 % ID/g; $^{64}$Cu-NOTA-1, 1.30±0.22 % ID/g; and $^{64}$Cu-BaBaSar-1, 11.20±1.17 % ID/g) demonstrated clearance with time (Online Resources ESM 1–4). $^{64}$Cu-DOTA-1 and $^{64}$Cu-NOTA-1 exhibited stable tumor/blood ratios (approximately 3–5) at all time points while $^{64}$Cu-CB-TE1A1P-1 exhibited an initial increase from 1 to 4 h p.i. (1 h—3.98±1.99, 4 h—8.25±1.49, $p$=0.041) that leveled off at 24 h p.i. Interestingly, $^{64}$Cu-BaBaSar-1 exhibited steady tumor/blood ratios from 1 to 4 h p.i., but a dramatically significant drop at 24 h p.i. (4 h—7.20±0.55; 24 h—0.77±0.26, $p$<0.0001) (Fig. 5d). Tumor/muscle ratios reveal that $^{64}$Cu-DOTA-1 was the only radiotracer to demonstrate an overall upwards trend through the time points (1 h—1.76±0.49, 4 h—2.76±0.63, 24 h—4.23±0.29), the others demonstrated fairly stable ratios at all three time points (Fig. 5e).

After a pre-injection of $NH_2$-$PEG_{28}$-A20FMDV2, all tracers except $^{64}$Cu-NOTA-1 showed a statistically significant reduction in binding to the positive tumor at 24 h p.i, $^{64}$Cu-CB-TE1A1P-1 (without blocking—0.89±0.21 % ID/g; with blocking—0.14±0.15 % ID/g, $p$=0.023), $^{64}$Cu-DOTA-1 (without blocking—1.28±0.30 % ID/g, with blocking—0.51±0.14 % ID/g, $p$=0.046), $^{64}$Cu-NOTA-1 (without blocking—0.98±0.31 % ID/g, with blocking—1.52±0.31 % ID/g, $p$=0.154), and $^{64}$Cu-BaBaSar-1 (without blocking—2.23±0.63 % ID/g, with blocking—0.69±0.03 % ID/g, $p$=0.046) (Fig. 5a).

### Urine Analysis

In urine, all radiotracers showed significant degradation at 1 h p.i. ($^{64}$Cu-CB-TE1A1P-1—1 % intact, $^{64}$Cu-DOTA-1—6.6 % intact as a double peak, $^{64}$Cu-NOTA-1—15.9 %, and $^{64}$Cu-BaBaSar-1—3 % intact). All four radiotracers demonstrated similar degradation in that they all showed the formation of a new, more polar metabolite with a 2–3 min faster retention time on radioHPLC than the parent radiotracer (Fig. 3b).

### Autoradiography and Histology

Autoradiography slices of the positive and negative tumor further confirm selective binding to the $\alpha_v\beta_6$-positive xenograft at all times with $^{64}$Cu-NOTA-1 exhibiting the smallest difference in uptake between the positive and negative tumors (Fig. 6a, b). The images reveal the majority of the uptake to be around the tumor margins. Immunohistochemistry staining of the positive tumor for the integrin $\alpha_v\beta_6$ confirmed high expression around the margins of the tumors with no expression at the necrotic core (Fig. 6c). Additional autoradiography slices of the kidney reveal uptake within the renal cortex (data not shown).

## Discussion

The integrin $\alpha_v\beta_6$ plays an important role in the imaging of cancer with PET [22]. Although not expressed in the majority of healthy adult epithelium, this integrin is upregulated in various cancers and serves as a prognosis indicator due to its overexpression in aggressive cancers [3, 7, 9]. Thus, it is desirable to have a non-invasive imaging probe to detect $\alpha_v\beta_6$-positive tumors as it can provide valuable information for both diagnostic and treatment planning. Here, we described the $^{64}$Cu radiolabeling of the pegylated A20FMDV2 peptide, a

peptide shown to target the integrin $\alpha_v\beta_6$, via four different chelators. CB-TE1A1P is a cross-bridged cyclam-based macrocycle featuring a phosphonate pendant arm that can readily complex copper(II) under mild conditions at high specific activity [18, 23]. DOTA and NOTA are two commercially available, widely used chelators for a variety of different small molecules [24]. BaBaSar is a carboxyl-functionalized sarcophagine cage chelator with two benzoic acid moieties that has been shown to radiolabel under mild conditions while exhibiting high stability *in vivo* [20].

All four tracers were successfully radiolabeled with copper-64 on $PEG_{28}$-A20FMDV2 in good radiochemical purity under mild conditions. However, CB-TE1A1P-1 required a higher temperature to radiolabel at greater than 95 % RCP. This could be due to slower kinetics of copper complexation after the carboxymethyl pendant arm was conjugated onto the peptide. Previously, this chelator was radiolabeled on the peptidomimetic LLP2A via a hydrophilic linker and was able to radiolabel after 60 min at room temperature [18]. We observed approximately 45 % RCP after 15 min at 37 °C indicating the ability to complex copper at the same temperature as other the chelator-conjugated A20FMDV2 peptides but demanding a longer incubation period.

It has previously been demonstrated that the addition of bulky chelators or prosthetic groups can affect the binding, internalization, and metabolism of receptor targeting peptides [25–28]. The *in vitro* cell binding and internalization assays revealed that all four radiotracers show binding directed towards the integrin $\alpha_v\beta_6$ with fairly comparable internalization levels, indicating that the addition of a chelator and the radiolabeling with $^{64}$Cu did not drastically affect the binding potential of the $PEG_{28}$-A20FMDV2 peptide.

The four radiotracers showed varied stability in serum and urine. In serum, all radiotracers showed significant degradation with new metabolites forming after 24 h. Since all four chelators were conjugated onto the peptide via a carboxylic acid moiety, no obvious differences exist to account for variability in their *in vivo* stability. The urine metabolite studies revealed that all radiotracers degraded in a similar fashion to the previously studied 4-[$^{18}$F]-fluorobenzoyl-$PEG_{28}$-A20FMDV2 ([$^{18}$F]-FBA-$PEG_{28}$-A20FMDV2) in that they degraded into one major metabolite that is more polar [21].

Although high positive-to-negative tumor uptake ratios were observed for $^{64}$Cu-CB-TE1A1P-1 and $^{64}$Cu-BaBaSar-1, there was significantly unexpected higher kidney uptake than $^{64}$Cu-DOTA-1 and $^{64}$Cu-NOTA-1. Previous studies with a derivative of BaBaSar called AmBaSar (a sarcophagine cage with one benzoic acid) and DOTA on a cyclic RGD peptide in a mouse malignant glioma model showed <5 % ID/g uptake in the kidneys [19]. When CB-TE1A1P was tested on the peptidomimetic LLP2A in comparison to CB-TE2A, both conjugates also demonstrated low kidney uptake levels (<5 % ID/g) [18]. Similarly, when CB-TE1A1P was tested on the somatostatin agonist Y3-TATE, the kidney uptake level remained consistently low at 5 % ID/g at all time points (up to 24 h p.i.) [23]. These previous instances of low kidney uptake all occur on tracers demonstrating high metabolic stability [29–31]. Since the urine metabolite data reveals one major radioactive metabolite for all four radiotracers in this study, it is likely that the metabolite is accumulating within the kidney. However, [$^{18}$F]-FBA-$PEG_{28}$-A20FMDV2 quickly clears from the kidney (1 h—

24.7±4.8 % ID/g, 4 h—2.7±0.8 % ID/g) [16]. This result shows that while the addition of a bulky chelator group onto the peptide is not drastically influencing its binding affinity, it is clearly affecting how the peptide behaves *in vivo* and the binding of the metabolites formed. To further emphasize this point, when $PEG_{28}$-A20FMDV2 was labeled using Al[$^{18}$F]-NOTA, which is equivalent to a [$^{18}$F]-chelate, the radiotracer also exhibits extremely high and increasing kidney uptake in a pancreatic tumor mouse model [32]. These data suggest that the addition of any chelator onto this peptide alters its pharmacokinetic behavior. At this time, the identity of the major metabolite of each radiotracer has not been confirmed but is likely to be a $^{64}$Cu-chelate-peptide fragment [33]. Future efforts are underway to stabilize the $PEG_{28}$-A20FMDV2 peptide.

To demonstrate specific binding *in vivo*, blocking studies with cold peptide were performed. A decrease in the uptake of the radiotracer by the positive tumor is usually observed, such as with the statistically significant difference observed with $^{64}$Cu-CB-TE1A1P-1, $^{64}$Cu-DOTA-1, and $^{64}$Cu-BaBaSar-1. However, $^{64}$Cu-NOTA-1 exhibited an increase in binding to the $\alpha_v\beta_6$-positive tumor. The increase in binding to the $\alpha_v\beta_6$-positive tumor with $^{64}$Cu-NOTA-1 was surprising and the cause of it is not immediately known. While there is precedent in the literature indicating that uptake in organs can be affected by the overall mass injected [34, 35], this needs to be further investigated before any conclusions can be drawn.

The tumor/blood ratio for $^{64}$Cu-BaBaSar-1 significantly dropped from 4 to 24 h p.i., indicating a dramatic increase in blood concentration. This was unexpected since $^{64}$Cu-BaBaSar-1 was the only radiotracer to have any fraction intact at 24 h in the urine. Since the liver uptake also shows an increasing trend, this could be attributed to free $^{64}$Cu being released by the chelator. While liver uptake was relatively low among all of the radiotracers, $^{64}$Cu-CB-TE1A1P-1 demonstrated the lowest liver uptake and was the only radiotracer whose liver uptake did not increase over time. This demonstrates the *in vivo* inertness of the $^{64}$Cu-CB-TE1A1P conjugate, as accumulation in the liver can be attributed to transchelation and binding of $^{64}$Cu to proteins such as superoxide dismutase [36]. $^{64}$Cu-NOTA-1 demonstrated the highest liver uptake. $^{64}$Cu-DOTA-1 was the only radiotracer to exhibit increasing tumor/muscle ratios; however, the absolute % ID/g numbers reveal this is an effect of muscle clearance rather than an increase in tumor accumulation.

This study aimed to find the ideal $^{64}$Cu chelator for the radiolabeling of $PEG_{28}$-A20FMDV2. While the choice of chelator can affect different properties such as stability and selectivity *in vivo*, some of the pharmacokinetic effects are clearly attributed to the peptide itself. Ultimately, notable differences exist with the addition of any chelator to this peptide in comparison to the [$^{18}$F]-peptide previously radiolabeled with the FBA prosthetic group.

## Conclusion

In summary, the peptide $PEG_{28}$-A20FMDV2 was evaluated and characterized with four chelators: CB-TE1A1P, DOTA, NOTA, and BaBaSar. Compared to the two commercially available chelators, the two newly developed chelators, CB-TE1A1P and BaBaSar, showed

improved specificity for the $\alpha_v\beta_6$-positive tumor when conjugated onto $PEG_{28}$-A20FMDV2, but they also showed the highest kidney retention. Previous data show this is an inherent property of the peptide metabolizing *in vivo*, but the effect is compounded by the addition of a chelator, as this alters the binding properties of the metabolite compared to the identical peptide labeled with a fluorine-18 prosthetic group such as FBA. All four radiotracers demonstrated relatively low liver uptake. The data suggests no clear "best candidate" for the $^{64}$Cu radiolabeling of A20FMDV2, but instead a trade-off between the different properties (e.g., stability, selectivity, pharmacokinetics, etc.) with no obvious effects of the individual chelators. There are several Cu(II) chelators available from commercial sources and reported in the literature, and there is continued development of new chelators, but clearly many factors influence the selection for radiolabeling and subsequent use as imaging or therapeutic agents. Future studies will focus on working with a stabilized version of the A20FMDV2 peptide to achieve lower kidney uptake and faster renal clearance. This work demonstrates that several $^{64}$Cu-radiolabeled A20FMDV2 radiotracers can successfully target the integrin $\alpha_v\beta_6$ and serve as an imaging agent.

## Supplementary Material

Refer to Web version on PubMed Central for supplementary material.

## Acknowledgments

The authors would like to acknowledge D.L. Kukis, L. Planutyte, J.Y. Fung, M. Jiang, and S.H. Hausner for their advice and technical support.

*Grant Support.* This research was supported by the Office of Science, United States Department of Energy, DE-SC0002061 and NCI 5R01 CA093375.

## References

1. Bates RC, Bellovin DI, Brown C, et al. Transcriptional activation of integrin β6 during the epithelial–mesenchymal transition defines a novel prognostic indicator of aggressive colon carcinoma. J Clin Invest. 2005; 115:339–347. [PubMed: 15668738]
2. Bruess JM, Gallo J, DeLisser HM, et al. Expression of the β6 integrin subunit in development, neoplasia and tissue repair suggests a role in epithelial remodeling. J Cell Sci. 1995; 108:2241–2251. [PubMed: 7673344]
3. Maubant S, Cruet-Hennequart S, Dutoit S, et al. Expression of α V-associated integrin β subunits in epithelial ovarian cancer and its relation to prognosis in patients treated with platinum-based regimens. J Mol Histol. 2005; 36:119–129. [PubMed: 15704006]
4. Sipos B, Hahn D, Carceller A, et al. Immunohistochemical screening for β6-integrin subunit expression in adenocarcinomas using a novel monoclonal antibody reveals strong up-regulation in pancreatic ductal adenocarcinomas *in vivo* and *in vitro*. Histopathology. 2004; 45:226–236. [PubMed: 15330800]
5. Saha A, Ellison D, Thomas GJ, et al. High-resolution in vivo imaging of breast cancer by targeting the pro-invasive integrin αvβ6. J Pathol. 2010; 222:52–63. [PubMed: 20629113]
6. Hazelbag S, Kenter GG, Gorter A, et al. Overexpression of the αvβ6 integrin in cervical squamous cell carcinoma is a prognostic factor for decreased survival. J Pathol. 2007; 212:316–324. [PubMed: 17503414]
7. Zhang ZY, Xu KS, Wang JS, et al. Integrin αvβ6 acts as a prognostic indicator in gastric carcinoma. Clin Oncol. 2008; 20:61–66.

8. Li X, Yang Y, Hu Y, et al. αvβ6-Fyn signaling promotes oral cancer progression. J Biol Chem. 2003; 278:41646–41653. [PubMed: 12917446]
9. Yang G-Y, Xu K-S, Pan Z-Q, et al. Integrin alphavbeta6 mediates the potential for colon cancer cells to colonize in and metastasize to the liver. Cancer Sci. 2008; 99:879–887. [PubMed: 18294287]
10. Elayadi AN, Samli KN, Prudkin L, et al. A peptide selected by biopanning identifies the integrin αvβ6 as a prognostic biomarker for nonsmall cell lung cancer. Cancer Res. 2007; 67:5889–5895. [PubMed: 17575158]
11. Gagnon MKJ, Hausner SH, Marik J, et al. High-throughput in vivo screening of targeted molecular imaging agents. Proc Natl Acad Sci U S A. 2009; 106:17904–17909. [PubMed: 19815497]
12. Hackel BJ, Kimura RH, Miao Z, et al. 18F-Fluorobenzoate–Labeled Cystine Knot Peptides for PET Imaging of Integrin αvβ6. J Nucl Med. 2013
13. Aina OH, Sroka TC, Chen M-L, Lam KS. Therapeutic cancer targeting peptides. Biopolymers. 2002; 66:184–199. [PubMed: 12385037]
14. Hausner SH, DiCara D, Marik J, et al. Use of a peptide derived from foot-and-mouth disease virus for the noninvasive imaging of human cancer: generation and evaluation of 4-[$^{18}$F]fluorobenzoyl A20FMDV2 for in vivo imaging of integrin alphavbeta6 expression with positron emission tomography. Cancer Res. 2007; 67:7833–7840. [PubMed: 17699789]
15. Hausner SH, Abbey CK, Bold RJ, et al. Targeted in vivo imaging of integrin $alpha_v beta_6$ with an improved radiotracer and its relevance in a pancreatic tumor model. Cancer Res. 2009; 69:5843–5850. [PubMed: 19549907]
16. Hausner SH, Kukis DL, Gagnon MK, et al. Evaluation of [$^{64}$Cu]Cu-DOTA and [$^{64}$Cu]Cu-CB-TE2A chelates for targeted positron emission tomography with an alphavbeta6-specific peptide. Mol Imaging. 2009; 8:111–121. [PubMed: 19397856]
17. Blower PJ, Lewis JS, Zweit J. Copper radionuclides and radiopharmaceuticals in nuclear medicine. Nucl Med Biol. 1996; 23:957–980. [PubMed: 9004284]
18. Jiang M, Ferdani R, Shokeen M, Anderson CJ. Comparison of two cross-bridged macrocyclic chelators for the evaluation of $^{64}$Cu-labeled-LLP2A, a peptidomimetic ligand targeting VLA-4-positive tumors. Nucl Med Biol. 2013; 40:245–251. [PubMed: 23265977]
19. Cai H, Li Z, Huang CW, et al. Evaluation of copper-64 labeled AmBaSar conjugated cyclic RGD peptide for improved microPET imaging of integrin αvβ3 expression. Bioconjug Chem. 2010; 21:1417–1424. [PubMed: 20666401]
20. Liu S, Li Z, Yap LP, Huang CW, et al. Efficient preparation and biological evaluation of a novel multivalency bifunctional chelator for $^{64}$Cu radiopharmaceuticals. Chemistry. 2011; 17:10222–10225. [PubMed: 21815227]
21. Hausner SH, Carpenter RD, Bauer N, Sutcliffe JL. Evaluation of an integrin alphavbeta6-specific peptide labeled with [$^{18}$F]fluorine by copper-free, strain-promoted click chemistry. Nucl Med Biol. 2013; 40:233–239. [PubMed: 23265667]
22. Nemeth JA, Nakada MT, Trikha M, et al. Alpha-v integrins as therapeutic targets in oncology. Cancer Invest. 2007; 25:632–646. [PubMed: 18027153]
23. Guo Y, Ferdani R, Anderson CJ. Preparation and biological evaluation of (64)Cu labeled Tyr(3)-octreotate using a phosphonic acid-based cross-bridged macrocyclic chelator. Bioconjug Chem. 2012; 23:1470–1477. [PubMed: 22663248]
24. Anderson CJ, Ferdani R. Copper-64 radiopharmaceuticals for PET imaging of cancer: advances in preclinical and clinical research. Cancer Biother Radiopharm. 2009; 24
25. Anderson CJ. Metabolism of radiometal-labeled proteins and peptides: what are the real radiopharmaceuticals in vivo? Cancer Biother Radiopharm. 2001; 16:451–455. [PubMed: 11789022]
26. Novak-Hofer I, Zimmermann K, Schubiger PA. Peptide linkers lead to modification of liver metabolism and improved tumor targeting of copper-67-labeled antibody fragments. Cancer Biother Radiopharm. 2001; 16:469–481. [PubMed: 11789024]
27. Zeglis BM, Lewis JS. A practical guide to the construction of radiometallated bioconjugates for positron emission tomography. Dalton Trans. 2011; 40:6168–6195. [PubMed: 21442098]

28. Hausner SH, Marik J, Gagnon MKJ, Sutcliffe JL. In vivo positron emission tomography (PET) imaging with an αvβ6 specific peptide radiolabeled using $^{18}$F-"click" chemistry: evaluation and comparison with the corresponding 4-[$^{18}$F]fluorobenzoyl- and 2-[$^{18}$F]fluoropropionyl-peptides. J Med Chem. 2008; 51:5901–5904. [PubMed: 18785727]
29. DeNardo SJ, Liu R, Albrecht H, et al. $^{111}$In-LLP2A-DOTA polyethylene glycol-targeting $\alpha_4\beta_1$ integrin: comparative pharmacokinetics for imaging and therapy of lymphoid malignancies. J Nucl Med. 2009; 50:625–634. [PubMed: 19289419]
30. Haubner R, Decristoforo C. Radiolabelled RGD peptides and peptidomimetics for tumour targeting. Front Biosci. 2009; 14:872–886.
31. Nguyen K, Parry JJ, Rogers BE, Anderson CJ. Evaluation of copper-64-labeled somatostatin agonists and antagonist in SSTr2-transfected cell lines that are positive and negative for p53: implications for cancer therapy. Nucl Med Biol. 2012; 39:187–197. [PubMed: 22056254]
32. Hausner SH, Bauer N, Sutcliffe JL. *In vitro* and *in vivo* evaluation of the effects of aluminum [$^{18}$F]fluoride radiolabeling on an integrin avb6-specific peptide. Nucl Med Biol. 2013; 41:43–50. [PubMed: 24267053]
33. Bass LA, Lanahan MV, Duncan JR, et al. Identification of the soluble in vivo metabolites of indium-111-diethylenetriaminepentaacetic acid-D-Phe1-octreotide. Bioconjug Chem. 1998; 9:192–200. [PubMed: 9548534]
34. Breeman WAP, Kwekkeboom DJ, Kooij PPM, et al. Effect of dose and specific activity on tissue distribution of indium-111-pentetreotide in rats. J Nucl Med. 1995; 36:623–627. [PubMed: 7699456]
35. Lewis JS, Lewis MR, Cutler PD, et al. Radiotherapy and dosimetry of 64Cu-TETA-Tyr3-octreotate in a somatostatin receptor-positive, tumor-bearing rat model. Clin Cancer Res. 1999; 5:3608–3616. [PubMed: 10589778]
36. Smith SV. Molecular imaging with copper-64. J Inorg Biochem. 2004; 98:1874–1901. [PubMed: 15522415]

CB-TE1A1P-**1**

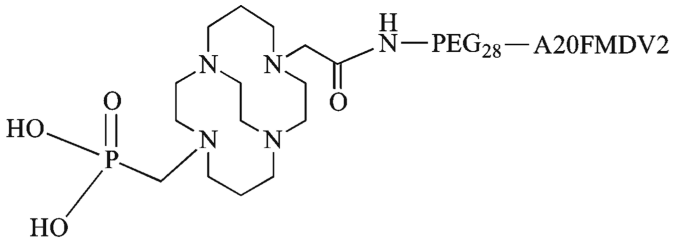


DOTA-**1**

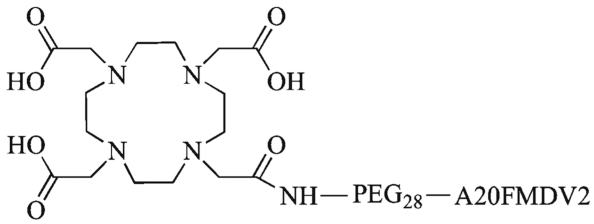


PEG$_{28}$ — A20FMDV2 =**1**

NOTA-**1**

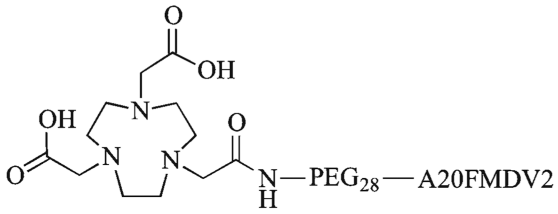


BaBaSar-**1**

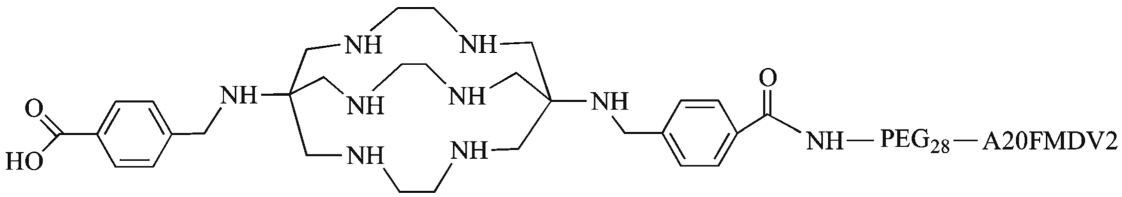


**Fig. 1.**

The four chelators conjugated to PEG$_{28}$-A20FMDV2.

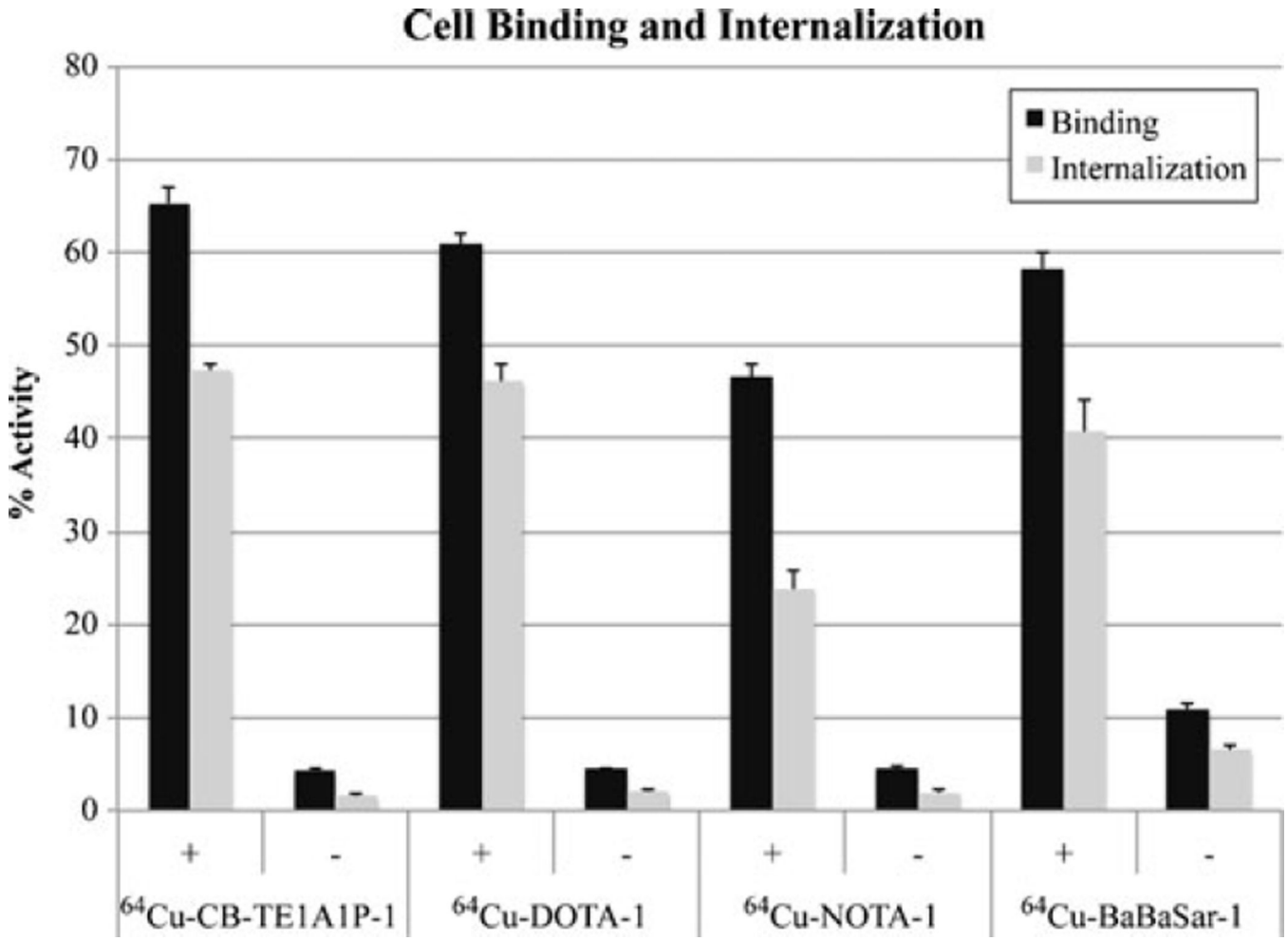


**Fig. 2.**

*In vitro* binding (*black*) and internalization (*gray*) results after 60 min using $\alpha_v\beta_6$-positive and $\alpha_v\beta_6$-negative cells. Internalization levels shown as percent relative to total activity.

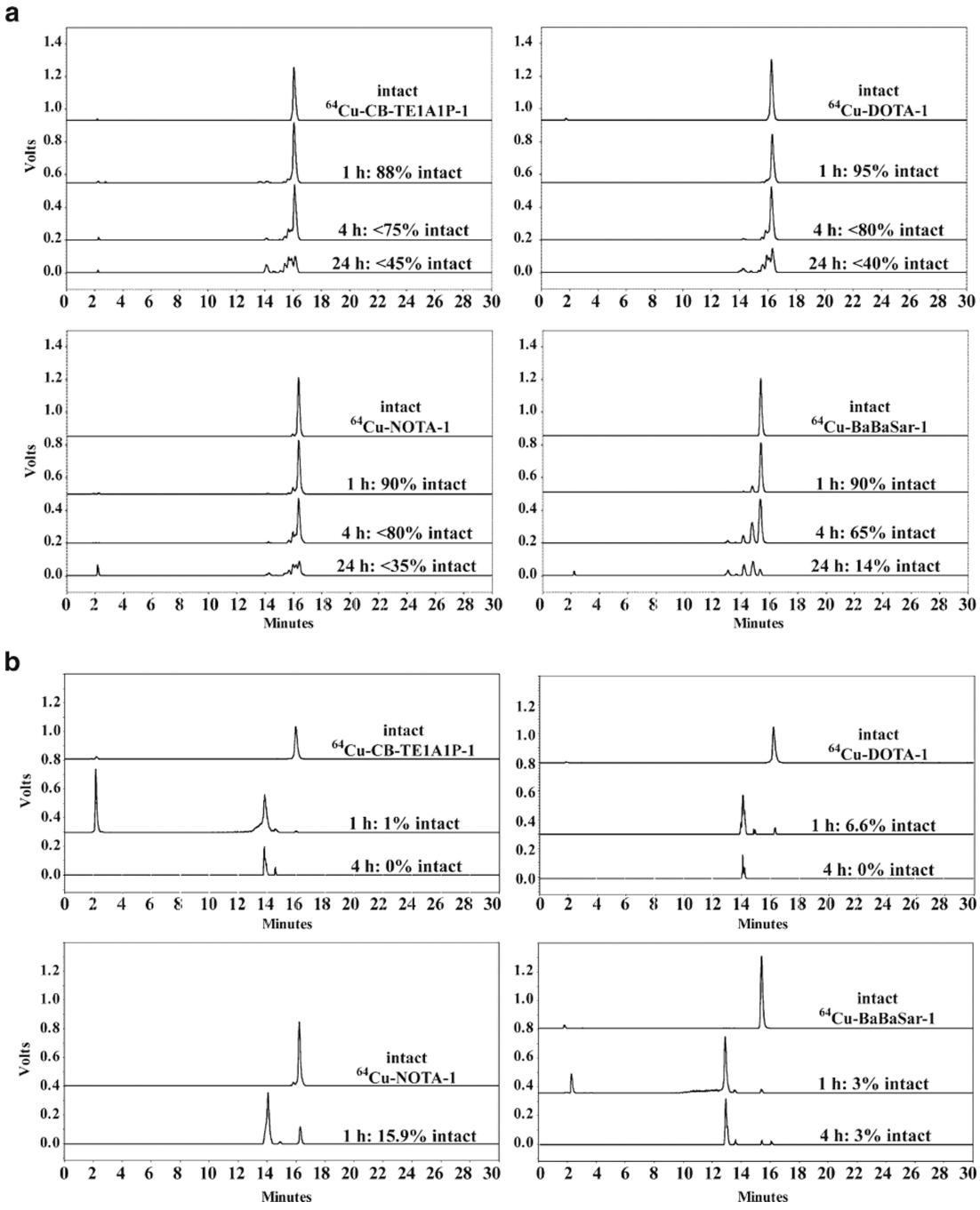


**Fig. 3.**

**a** Serum stability HPLC traces for each radiotracer after incubating in mouse serum for 1, 4, and 24 h (*top to bottom* for each radiotracer); **b** urine metabolite HPLC traces after 1 and 4 h p.i. for each radiotracer (unable to collect urine sample for $^{64}$Cu-NOTA-1 at 4 h p.i.).

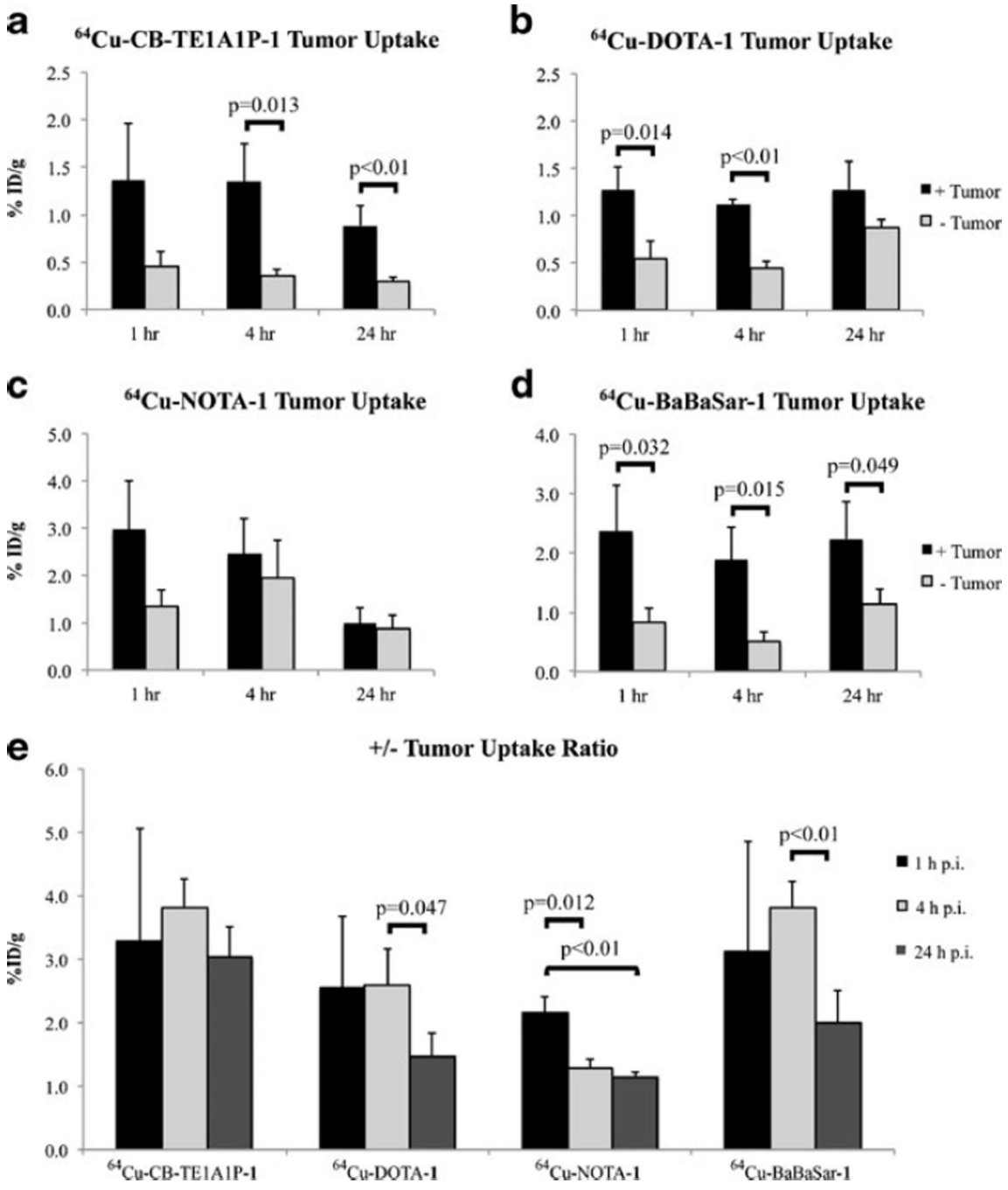


**Fig. 4.**

Uptake in the (+) and (−) tumors as determined by biodistribution studies at 1, 4, and 24 h p.i. for **a** $^{64}$Cu-CB-TE1A1P-1, **b** $^{64}$Cu-DOTA-1, **c** $^{64}$Cu-NOTA-1, and **d** $^{64}$Cu-BaBaSar-1 (individually scaled). These values were used to calculated **e** positive to negative tumor uptake ratios. Uptake values are represented as % ID/g. *P* values were determined using paired, two-tailed Student *t* tests.

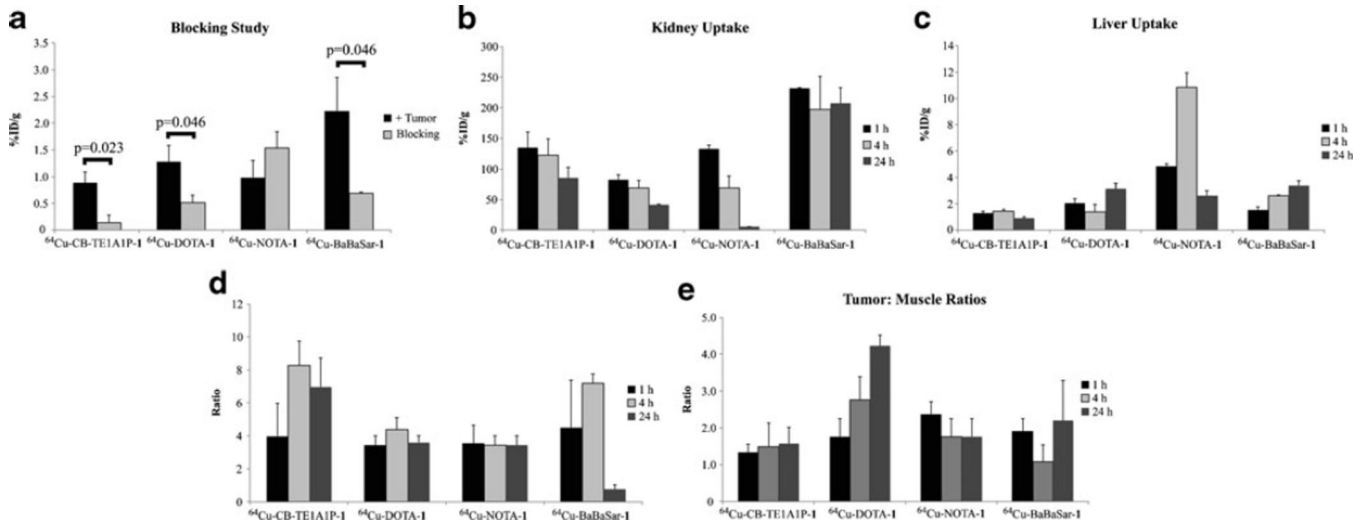


**Fig. 5.**

**a** Blocking study results with an injection of $NH_2$-$PEG_{28}$-A20FMDV2 10 min prior to injecting the formulated radiotracers. Uptake in the key organs **b** kidney and **c** liver at 1, 4, and 24 h p.i.; **d** tumor to blood and **e** tumor to muscle ratios at 1, 4, and 24 h p.i. Uptake values are represented as % ID/g with *n*=3/radiotracer per experiment per time point.

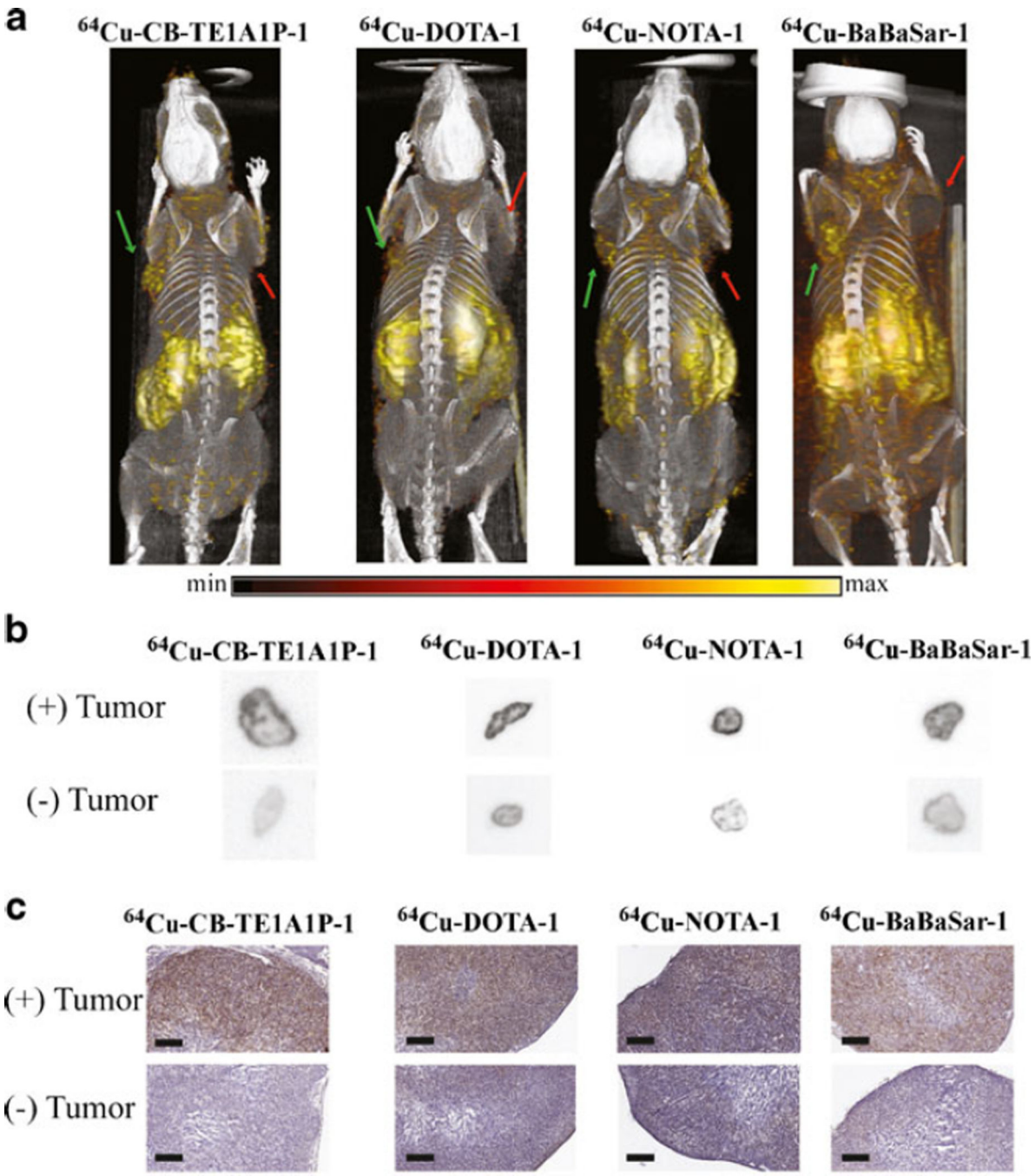


**Fig. 6.**

**a** Reconstructed 3D PET/CT images showing (+) (*green arrow*) and (−) (*red arrow*) tumors. Mice were anesthetized using 2–3 % isoflurane and received 150–250 μCi of formulated radiotracer via tail vein. All images were acquired 4 h p.i. using 20 min static scans. **b** Autoradiography slices (20 μm) of (+) and (−) tumors, sectioned at 4 h p.i. and exposed overnight. Each slice read at a 50-μm resolution. **c** Histology slices (5 μm) from (+) and (−)

tumors after immunohistochemistry staining for $\alpha_v\beta_6$ viewed at ×4 magnification. *Scale bar* = 400 μm.

**Table 1**

Analytical data and reaction parameters for the four radiotracers

| | $^{64}$Cu-CB-TE1A1P-1 | $^{64}$Cu-DOTA-1 | $^{64}$Cu-NOTA-1 | $^{64}$Cu-BaBaSar-1 |
|---|---|---|---|---|
| Molecular weight (unlabeled compound) | 3,827.3 | 3,852.1 | 3,752.2 | 4,031.9 |
| Calculated molecular weight (unlabeled compound) | 3,827.5 | 3,852.2 | 3,752.3 | 4,031.8 |
| Reaction temperature | 50 °C | 37 °C | 37 °C | 37 °C |
| Radiochemical purity | 98 % | 95 % | 96 % | 97 % |
| Specific activity (Ci/μmol) | 0.58 | 0.59 | 0.58 | 0.60 |

**Table 2**

A summary of results from *in vitro* and *in vivo* studies

| | $^{64}$Cu-CB-TE1A1P-1 | $^{64}$Cu-DOTA-1 | $^{64}$Cu-NOTA-1 | $^{64}$Cu-BaBaSar-1 |
|---|---|---|---|---|
| Serum stability (24 h) | <45 % | <40 % | <35 % | 14.0 % |
| Urine metabolites (%intact at 4 h) | 0 % | 0 % | – | 3 % |
| Positive tumor uptake (4 h) | 1.34±0.40 % ID/g | 1.11±0.58 % ID/g | 2.44±0.76 % ID/g | 1.88±0.55 % ID/g |
| Positive/negative tumor uptake ratio | 3.82±0.44 % | 2.58±0.58 % | 1.29±0.14 % | 3.82±0.41 % |
| Liver uptake (4 h) | 1.45±0.14 % ID/g | 1.41±0.57 % ID/g | 10.83±1.1 % ID/g | 2.61±0.05 % ID/g |
| Kidney uptake (4 h) | 122.7±25.8 % ID/g | 69.18±11.8 % ID/g | 69.12±19.5 % ID/g | 196.9±54.5 % ID/g |